ANL/EXT-09-25

Candidate Materials and Potential In-service Degradation Issues for Steam Generator in the Primary Loop of Next Generation Nuclear Plant

S. Majumdar, A. Moisseytsev, and K. Natesan
Nuclear Engineering Division

September 2009

Argonne National Laboratory
Argonne, IL 60439

Sponsored by the Idaho National Laboratory
for the U.S. Department of Energy
Office of Nuclear Energy, Science, and Technology

Argonne is operated by UChicago Argonne, LLC
under DOE Contract DE-AC02-06CH11357.

Executive Summary

The NGNP, which is an advanced HTGR concept with emphasis on both electricity and hydrogen production, involves helium as the coolant and a closed-cycle gas turbine for power generation with a core outlet/gas turbine inlet temperature of 900-1000°C. In the indirect cycle system, an intermediate heat exchanger is used to transfer the heat from primary helium from the core to the secondary fluid, which can be helium, nitrogen/helium mixture, or a molten salt. The system concept for the VHTR can be a reactor based on the prismatic block of the GT-MHR developed by a consortium led by General Atomics in the U.S. or based on the PBMR design developed by ESKOM of South Africa and British Nuclear Fuels of U.K.

This report has reviewed the available information on candidate materials for the construction of steam generator for application in NGNP and has made a preliminary assessment of several relevant factors and presents options for the selection of material for steam generator application. In addition, Thermal conduction and basic pressure and thermal stress analyses of two of the hottest 360°-turn coils of the SG/superheater have been conducted. The stresses were compared to the allowables of Subsection NH of the ASME Code. The primary stresses in the Alloy 800H superheater limit its creep rupture design life to 3 X 10^5 h. The primary stresses in the 2-1/4Cr-1Mo SG limit its creep rupture design life to 10^5 h. Both the SG and the superheater satisfy the ratcheting strain limit of Subsection NH.

In future, all the coils of the SG need to be included in the FEM. Their inclusion would lower the highest temperatures calculated for the coils in the present report since it would allow heat conduction to occur in the axial direction of the helix. However, the effect should be small because convective heat transfer through the coolant dominates the conductive heat transfer through the tube wall.

Contents

Acronyms

AVB	Anti Vibration Bar
AVT	All Volatile Treatment
DOE	Department of Energy
EPRI	Electric Power Research Institute
FEM	Finite Element Modeling
FIV	Flow Induced Vibration
GT-MHR	Gas Turbine - Modular Helium Reactor
HCHX	Helical Coil Heat Exchanger
HCSG	Helical Coil Steam Generator
HTC	Heat Transfer Coefficient
HTGR	High Temperature Gas Reactor
IGA	Intergranular Attack
IGSCC	Intergranular Stress Corrosion Cracking
IHX	Intermediate Heat Exchanger
LWR	Light Water Reactor
MA	Mill Annealed
NGNP	Next Generation Nuclear Plant
OTSG	Once Through Steam Generator
PBMR	Pebble Bed Modular Reactor
PWR	Pressurized Water Reactor
R&D	Research and Development
RSG	Recirculating Steam Generator
RTZ	Roll Transition Zones
SCC	Stress Corrosion Cracking
TGSCC	Transgranular Stress Corrosion Cracking
TS	Tube Sheet
TSP	Tube Support Plate
VHTR	Very High Temperature Reactor System

Candidate Materials and Potential In-service Degradation Issues for Steam Generator in the Primary Loop of Next Generation Nuclear Plant

1. Introduction

In the coming decades, the United States and the entire world will need energy supplies to meet the growing demands due to population increase and increase in consumption due to global industrialization. One of the reactor system concepts, the Very High Temperature Reactor (VHTR), with helium as the coolant, has been identified as uniquely suited for producing hydrogen without consumption of fossil fuels or the emission of greenhouse gases [Generation IV 2002]. The U.S. Department of Energy (DOE) has selected this system for the Next Generation Nuclear Plant (NGNP) Project, to demonstrate emissions-free nuclear-assisted electricity and hydrogen production within the next 15 years.

The NGNP reference concepts are helium-cooled, graphite-moderated, thermal neutron spectrum reactors with a design goal outlet helium temperature of ≈1000°C [MacDonald et al. 2004]. The reactor core could be either a prismatic graphite block type core or a pebble bed core. The use of molten salt coolant, especially for the transfer of heat to hydrogen production, is also being considered. The NGNP is expected to produce both electricity and hydrogen. The process heat for hydrogen production will be transferred to the hydrogen plant through an intermediate heat exchanger (IHX).

The basic technology for the NGNP has been established in the former high temperature gas reactor (HTGR) and demonstration plants (DRAGON, Peach Bottom, AVR, Fort St. Vrain, and THTR). In addition, the technologies for the NGNP are being advanced in the Gas Turbine-Modular Helium Reactor (GT-MHR) project, and the South African state utility ESKOM-sponsored project to develop the Pebble Bed Modular Reactor (PBMR). Furthermore, the Japanese HTTR and Chinese HTR-10 test reactors are demonstrating the feasibility of some of the planned components and materials.

One of the current approaches is to use conventional steam generators to transfer heat from the helium to the steam that can used to drive a turbine for power generation. However, the steam generator in the NGNP will be somewhat different due to the high helium temperatures and pressures in the secondary reactor circuit. In addition, the since the gas heat transfer coefficients are generally much smaller than that of water, a large surface area is required to transfer the thermal load. For this purpose, a helical coil design is envisioned for the steam generator. This report is an attempt to examine the thermal hydraulics and steam generator materials performance in a helical coil steam generator. The calculated results on the stresses are compared to the ASME Section III Subsection NH values for assessing Code compliance.

2. Background

In pressurized water reactors (PWRs) in the US, the primary coolant removes the heat generated from the reactor core. Each primary coolant loop has one vertically mounted steam generator (SG). Typically, each plant has two to four reactor coolant loops. The hot primary coolant enters and leaves the SG through nozzles in the hemispherical lower head of the SG. A divider plate in the lower head keeps the hot incoming coolant separated from the cooler

outgoing coolant. The SG tubes provide the primary means by which heat is transferred from the primary system water to the water on the secondary side. The primary coolant is then returned to the reactor core via the coolant pump and the cycle is repeated.

Feedwater (secondary coolant) is pumped into the secondary side (shell side) of the SG where it boils into steam. The steam exits the SG through an outlet nozzle and flows to the turbine generator, where it spins the turbine, generating electricity. After exiting the turbine, the steam is condensed back into water and pumped back into the SG, where the cycle is repeated.

SG tube surfaces constitute more than 50% of the primary coolant pressure boundary in a PWR. This pressure boundary is an important element of the defense in depth against a release of radioactive materials from the reactor into the environment. Unlike the pressure boundary of other primary components (e.g., hot leg, surge line, etc.), the barrier to fission product release provided by the SG tube surfaces is not reinforced by the reactor containment. Any fission product released through a leaking or ruptured tube can escape directly into the environment through the secondary side of the SG (i.e., bypass the containment). Therefore, the integrity of the SG tubes must be ensured with high confidence.

In order to maintain structural and leakage integrity of the SG tubes with adequate margins, inservice inspections are conducted at regular intervals. These inspections are adequate to detect degradation at a sufficiently early stage to preclude the progression of the degradation to the point that the regulatory criteria regarding SG tube structural and leakage integrity can no longer be met during the interval between the inspections.

From the point of view of the utility, maximizing the inspection interval without jeopardizing tube integrity is an important economic goal. One important tool at the disposition of the utility to achieve this goal is to select a tube material that is structurally strong (i.e., has high mechanical strength and has high resistance to corrosion), has good thermal properties and is amenable to inspection by NDE (typically eddy current testing). Historically several materials have been used in the nuclear industry that fit these requirements to various degrees. They are

1) Austenitic stainless steels
2) Alloy 600
3) Alloy 800
4) Alloy 690

Among 69 currently operating PWRs in the US, approximately, 25% use thermally treated Alloy 600 and 43% use thermally treated Alloy 690, as of December 2004 (Karwoski et al 2007). Although the rest use mill-annealed Alloy 600 tubes, their numbers are decreasing with time as the older SGs are being replaced by newer SGs using either Alloy 600TT or Alloy 690TT tubes. Alloy 800 tubes have been used in Germany, Spain and Canada, but none in the US PWRs. Table 1 provides a relative ranking of the corrosion resistance of various tubing alloys subjected to a range of chemical environments (Harrod et al 2001). Alloy 690TT is generally considered immune to primary water stress corrosion cracking (PWSCC), and the data in Table 1 shows that Alloy 690TT exhibits equal or superior SCC resistance to other candidate SG tubing alloys in the environments of interest. The thermal conductivity of Alloy 690TT is lower than that of Alloy 600 but higher than that of Alloy 800, and ranks equally with other candidate alloys with respect to availability, manufacturability, and inspectability. It is more expensive than Alloy 800 and austenitic stainless steels and slightly more expensive than Alloy 600. Weld filler metals (Alloys 52 and 152) for Alloy 690TT have been developed, qualified, and used successfully by all SG manufacturing vendors.

Table 1. Relative Ranking of Corrosion Resistance of Candidate SG Tubing Alloys

	Alloy 600		Alloy 690	Alloy 800	304 SS
Corrosion Issue/environment	MA	TT	TT	MOD	-
Stress Corrosion Cracking					
Chloride					
Acid	1	1	1	2-3	(4)
Acid+SO_4(trace)	2-3	2	1	(1-2)	(3)
Neutral (or AVT)	1	1	1	2	5
Caustic					
Below 6%	3	2	1	2	5
10-50%	4	2	2	3	5
Water					
Pure, primary & AVT w/H_2	4	2-3	1	1	1
Pure w/O_2	4	3	1	(2)	5
Sulfur Compounds					
Acid sulfate	3	1	1	2	5
Alkaline sulfate	1	1	1	(1)	(2)
Acid-reduced compounds	3-4	2	(1)	(2)	(4)
Alkaline-reduced compounds	2	(3)	3	3	(5)
Lead-containing environments					
Acid	4	4	1	3	(4)
Neutral (or AVT)	3-4	3	1	1	1
Alkaline	3-4	3	4-5	5	5
Intergranular Attack (IGA)					
Acid	3-4	2-3	1-2	(4-5)	(4-5)
Alkaline	4	2	1	4	(5)
Pitting in Chlorides	3-4	3-4	2	3	4
Wastage					
Phosphates	3	(3)	(2)	(2)	3
Sulfates	3	3	2	2	1

Rankings: 1 - Best; 5- Worst; ( ) Estimates
MA - Mill Annealed; TT - Thermally Treated

2.1 Alloy 600

2.1.1 Review of US PWR Steam Generator (SG) Experience

Corrosion in steam generators has been a problem since the very introduction of pressurized water reactor (PWR) technology. The first recorded instance of stress corrosion cracking (SCC) of Alloy 600 was reported (LaQue 1957) as intergranular SCC (IGSCC) of a single tube from the water side near the tube sheet (TS) of a heat exchanger that was operating at 550°F. Shippingport, the first commercial PWR operated in the United States, developed leaking cracks in two Type 304 stainless steel (SS) steam generator tubes as early as 1957, after only 150 h of operation (Singley et al 1959, Welinsky et al 1968, Cheng 1975). The cracks were attributed to SCC that was produced by free caustic in the secondary water and steam that blanketed the tubes at the top inlet portion of the steam generator, leading to concentration of the caustic. The leaking tubes were plugged, and the addition of sodium phosphate was instituted to control the pH of the secondary water. Other early incidents of SCC in austenitic SS steam generator tubes occurred at the Savannah River Heavy Water Plutonium Production

Reactor in 1960 McKane et al 1960), the USS Nautilus reactor (Berry et al 1960), the Hanford New Production Reactor in 1963 (Kratzer 1971), the Yankee Rowe PWR in 1966-69 (Bush and Dillon 1973, Wagner 1970), and the Indian Point Unit 1 PWR in 1968 (Wagner 1970). The first three failures were attributed to halide–inducted SCC and the latter two to free caustic.

Because austenitic SS steam generator tubes were found to be susceptible to SCC by both chlorides and free caustic, the decision was made in the late 1950s to use Alloy 600 tubes in the United States and most of Europe, and Alloy 800 tubes in Germany, Spain, and Canada (Gras 1992). However, these changes did not eliminate corrosion-related tube degradation in steam generators. As shown in Fig. 1, a succession of failure processes has continued to afflict steam generators in the United States since the widespread use of Alloy 600 tubing in the late 1960s (Tapping 2006, EPRI 2000, Steam Generator Owners Group 1985). Essentially similar failure processes have also been experienced around the world. However, to this date, the exact mechanisms for SCC of Alloy 600 in deaerated high-temperature water remain elusive (Majumdar 1999).

Prior to the publication of a seminal paper by Coriou et al (1959), the general belief in the PWR steam generator community, based on hundreds of laboratory tests (Copson and Berry 1962), was that Alloy 600 tubing was immune to IGSCC when exposed to high-purity deaerated water at high temperature. The occasional SCC failures of PWR steam generator tubes during these early years were attributed to impurities such as caustic, lead compounds, etc. The results of Coriou et al were not confirmed by other investigators for almost 10 years. Later, however, many other laboratory tests have confirmed that depending on microstructure and processing history, Alloy 600 can and does experience IGSCC when exposed to aerated or deaerated high-temperature high-purity water.

The evolution of IGSCC-related problems in the steam generator tubes in the primary and the secondary sides differs because, although the bulk water in both the primary and the secondary sides of PWR's is pure and deaerated with dilute additives to control pH, impurity concentration processes can significantly alter the local chemical environment in the top of the tube sheet (TTS) and in tube support plate (TSP) crevices, and under sludge piles on the secondary side, where IGSCC occurs. Hence, the IGSCC mechanisms that operate in these two types of environments differ substantially. The primary environment consists of lithium hydroxide-buffered borated water, with hydrogen overpressure to remove oxygen that is formed by radiolysis. Concentration of boric acid is set by the requirements for reactivity control and ranges from 1800 ppm boron at the beginning of a cycle for high-burnup fuel to essentially 0 ppm boron at the end of the cycle. Lithium hydroxide is added to establish slight alkalinity. The pH in typical primary water ranges between 6.9 and 7.4 (PWR Guidelines 1990). During normal operation, the reactor coolant is at 305-330°C when it enters the primary side of a recirculating PWR steam generator and at 288-293°C during normal operation when it exits.

The chemistry of the secondary water is more complex and has evolved over the years as the industry experienced various types of corrosion on the secondary side. An early secondary-side corrosion problem for steam generators with Alloy 600 tubes was wastage, as indicated in Fig. 1. This problem was associated with the widely used coordinated sodium phosphate water chemistry (trisodium and disodium phosphate plus an oxygen scavenger such as sodium sulfite or hydrazine). The wastage was attributed to the development of corrosive phosphate solutions in regions of dryout, and the problem was controlled when almost all plants converted to an all-volatile ammonia-hydrazine secondary water treatment (AVT). This changeover was essentially completed in 1974, and wastage problems declined dramatically over the next two years (Fig. 1). However, tube denting at TSPs then became a significant problem, primarily in units with

copper alloy condensers cooled by sea or brackish water. Unlike the phosphate water chemistry, AVT provides no buffering against the local formation of highly acidic or alkaline conditions associated with impurity intrusion. The denting problem, caused by corrosion of the TSPs and the associated volume expansion of the corrosion products, was eventually alleviated by the addition of boric acid and better controls on impurity ingress.

Although most US plants discontinued the use of phosphate water chemistry in the mid-70's, San Onofre 1 and Robinson 2 continued its use. In both cases, some wastage and SCC

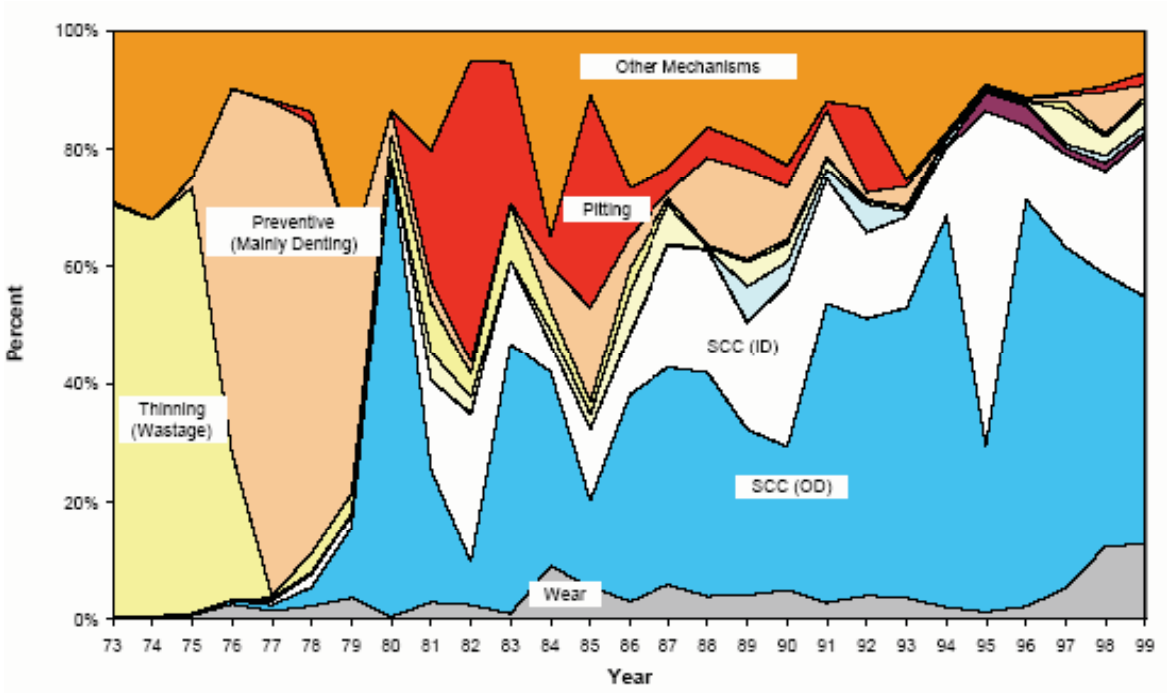

Figure 1. Causes of Steam Generator tube plugging history in the U.S. (Tapping 2006, EPRI report 2000).

continued to occur, ultimately leading to early retirement of San Onofre 1 in 1992 and SG replacement at Robinson 2 in 1984 (at which time the plant switched to AVT).

With time, however, more and more steam generator tubes began to exhibit IGSCC that was reminiscent of the earlier experience when AVT was used. This spurred R&D activities worldwide to investigate the causes and evaluate potential remedies for IGSCC. Historically, secondary water chemistry has been maintained within purity limits established by individual operating utilities. The purity levels that are maintained are functions of cooling water composition, secondary plant material and design, availability of full-flow condensate polishers, blowdown system capacity, and various other factors. Until recently, typical composition of recirculating steam generator (RSG) secondary water was chloride, (≤30 ppb); phosphate, 2-3 ppm; Na/PO_4 molar ratio, 2.0; dissolved oxygen, ≈10 ppb; hydrazine ≈20 ppb; copper, ≈2 ppb; iron, ≈20 ppb; conductivity, ≤50 mS-cm; and pH, 8.8 to 9.5 (Steam Generator Reference Book 1994). On-line addition of boric acid has sometimes been recommended to alleviate intergranular attack (IGA)/SCC at TSPs by possibly partially neutralizing caustics and providing a thicker, and more tightly adherent borate-containing film on the alloy (Paine et al 1988). Because operation of plants at these very low feedwater and/or blowdown impurity concentrations did not ensure the absence of steam generator tubing corrosion, Revision 3 of

Electric Power Research Institute (EPRI) water chemistry guidelines (PWR secondary water guidelines 1993) recommended an increase in feedwater hydrazine to >100 ppb, a decrease in feedwater iron concentration to 5 ppb, addition of boric acid, and consideration of controlling molar (cation to anion) ratio to establish a less aggressive (neutral to slightly acidic) crevice chemistry.

Historically, the earliest SCC cases in Alloy 600 steam generator tubing worldwide occurred somewhat rapidly on the secondary side. The degradation process involved the concentration of corrosive chemicals (e.g., NaOH, acid sulfates, etc.) in areas of limited coolant flow (crevices), e.g., tube/tube sheet (TS) junctions. Green and Paine (1981) reported incidences of outer-diameter (OD)-initiated SCC unrelated to crevice corrosion at the upper TS of a once-through steam generator (OTSG). Secondary side cracking has also been observed along scratches or lines of abrasion in free spans (e.g., SGs in McGuire, Oconee, and Farley). Secondary side SCC occurs in many forms and has always been responsible for a significant fraction of tubes that are plugged annually both in France (Gras 1992) and in the U.S. In the U.S. (Welty and Blomgren 1990), the first steam generator replacement was at Surry 2 in 1980 and was the result of denting. The first replacement of a steam generator due to secondary side IGA occurred in 1984 (Welty and Blomgren 1990).

Beginning in the early 1970s, Alloy 600 tubing was affected by another form of the IGSCC phenomenon, this time occurring on the primary side in highly stressed areas such as the roll transition zones (RTZs), inner-row U-bends, and subsequently at TSPs. This phenomenon was responsible for the greatest number of pluggings during mid to late 1970s (denting) and 1980s (primary-water SCC [PWSCC]) in the U.S. (Welty and Blomgren 1990) and during the 1980s (PWSCC) in France; it also was the cause for the first replacement of a steam generator in France in 1990 (Gras 1992). Similar replacements have also been carried out in Belgium, Spain, Sweden, and Japan.

In recent years, denting-related cracking has been controlled by improved secondary water chemistry, and inner-row U-bend cracking has been controlled by improved in-situ stress relief or by preventive plugging of susceptible tubes. Currently, SCC/IGA (OD) at the TSPs and TTS, where chemical concentration can occur, and PWSCC in expansion zones continue to be the major cause of IGSCC-related damage in steam generator tubing. Also, transgranular SCC (TGSCC) has been observed on the secondary side because of lead contamination (McKane et al 1960).

A large number of tubes (>10%) have required repair because of pitting in Indian Point 3 and Millstone 2, both using mill-annealed Alloy 600 tubes and salt water cooled condensers. The pitting has occurred primarily under sludge piles on the tube sheets, with the cold leg being affected more severely than the hot leg. The pitting is attributed to the presence of chlorides from cooling water in-leakage, relatively high concentrations of oxygen in the condensate, and the ingress of copper oxides and copper ions into the SGs. The pitting was a factor for replacing Indian Point 3 and Millstone 2 SG units. Moderate pitting (1-10% tubes repaired) has occurred in Connecticut Yankee, Indian Point 2, and Yankee Rowe, all using Alloy 600 MA except for Yankee Rowe which uses Type 304 stainless steel tubes. All used phosphate water chemistry for a while before switching to AVT and mainly suffered pitting during the AVT period. Although Indian Point 2 uses salt water cooling, the other two use fresh water cooling. Minor pitting (<1% tubes repaired) has occurred in Byron 1, Salem 2 and Trojan, all using Alloy 600 MA and AVT water chemistry. Salem 2 uses salt water cooling, the other two use fresh water cooling.

There have been two confirmed cases of U-bend fatigue in recirculating (RSG) type PWR SGs in the US. In North Anna 1, the fatigue was in the cold leg and was attributed to improper tube support leading to high flow-induced cyclic stresses. At Indian Point 3, the cracking occurred in the hot leg, in a properly supported U-bend. In this case, initiation of the fatigue crack was associated with shallow IGA/SCC at a dented TSP of the drilled hole type. In both cases, cracking occurred above the dented TSPs. It is suspected that denting causes reduction in damping, which leads to increased vibration amplitude and higher mean stress, both of which are conducive to fatigue crack initiation. The stress field generated by denting increases the likelihood of circumferential cracking. By and large, U-bend fatigue problem in the US RSGs is currently minor compared to IGSCC.

Although most cracking problems in the US have occurred in the tube sheet, tube support plate and U-bend areas, free-span cracking, though uncommon, is not rare. Free span cracks are not discussed in the literature because the tubes containing free span cracks are generally plugged upon detection. One tube rupture (in mid 90s), one large leak, and several large cracks have been observed in McGuire 1 and 2 due to IGSCC in the cold leg areas. Hundreds of cracks were initiated along the lines of abrasion on the tube OD created during installation. In 1993, a tube rupture occurred at Palo Verde 2. Investigation showed that the rupture was due to a long axial IGSCC in a free span area high in the tube bundle. Scratches on the tube surface are believed to have aggravated the situation by promoting initiation of cracks along a long length.

To summarize, most of the cracking currently suffered by Alloy 600 tubes of PWR steam generators is intergranular and three main types of intergranular attacks have been identified. Intergranular stress corrosion cracking/PWSCC occurs in the primary side mainly in the RTZs of the expanded tubes. On the secondary side, IGSCC, known as outer-diameter SCC (ODSCC), occurs typically in the crevices at the junctions of tubes with TS's and TSPs and under sludge piles, and IGA has been observed under sludge piles as well as at the tube to TSP junctions. Outer-diameter-initiated cracking can also occur from scratches or lines of abrasion in free spans.

2.1.2 Review of CANDU Steam Generator Experience

Within the Canadian fleet, only Bruce A and Bruce B SGs use Alloy 600 tubes. The early years of operation of CANDU reactors has been recently reviewed by Tapping (Tapping 2006). With the exception of the Douglas Point reactor, the period was characterized by relatively few operational problems associated with steam generators. During the same period PWR reactor steam generators (SGs) were experiencing tube degradation associated with denting of tubes at intersections with drilled hole support plates; followed by other forms of corrosion-related degradation. Figure 1 shows the evolution of the various SG degradation mechanisms observed to date with time for the first 30 years of operation, with stress corrosion cracking (SCC), either primary side SCC (IDSCC) or secondary side SCC (ODSCC) dominating the degradation. This history is essentially that of degradation of SGs tubed with Alloy 600. CANDU SG degradation experience with SGs tubed with Alloy 600 (Bruce A and B) has followed this PWR experience. No cracking has been detected at Bruce B after ≈20 years of operation, although some localized intergranular attack (IGA) has been detected. For PWRs SG degradation has accounted for about 0.3% of in-service tubes being plugged per year, on average, and for significant impact on capacity factors until recently. Thus, there has been a history or legacy of SG degradation, dominated by Alloy 600 issues, that has affected operation of all types of SGs, and has impacted regulatory and design decisions, as well as operational practices.

U-bend fatigue was first observed in CANDU SGs in a few tubes (Alloy 600) in Bruce A in 1978 with additional cases occurring in the late 70's and early 80's. The cracking was attributed to flow-induced vibration (FIV), with corrosion playing no significant role. Measures taken to mitigate the FIV problem kept the Bruce A SGs free from cracking up to about 1990. However, in mid-90's U-bend stress corrosion cracking reappeared at the U-bend restraint areas (stacked C-steel scallop bars). The tube-to-scallop bar holes are similar to holes in drilled tube support plates (TSPs) but have tapers at each end, with the central constant diameter cylindrical hole being 1/8 in. (3 mm) long. The tube-to-scallop bar holes were filled with deposits (TSP flow holes were 80% blocked), which extended above the scallop bars along the tube. IGA/IGSCC occurred under the deposits and the cracks were circumferential in orientation. At approximately the same time, the effects of lead contamination on the Bruce A Unit 2 steam generator became evident. At Bruce A Unit 2 the extent of lead-induced stress corrosion cracking, and lead contamination, was such that the unit was shut down in September 1995. Later, sludge pile pitting was discovered at Pickering-1 (Monel 400 SG tube), and fretting became a concern at Bruce-B. Repeated detection of fretting wear also indicated that the fabrication approach of some CANDU steam generators increased susceptibility to fretting damage in the U-bends. At Bruce-A, anti-vibration bars (AVBs) were added to stabilize the structure to reduce the risk of mechanical fatigue, stress corrosion cracking, and corrosion fatigue. Similarly, at Bruce-B, the installation of AVBs was required to reduce fretting degradation.

2.2 Alloy 690

Persistent issues of corrosion degradation, both on the tube inner diameter (ID) [primary water stress corrosion cracking (PWSCC)] and OD [intergranular attack (IGA) and stress corrosion cracking (SCC)] surfaces led to efforts to optimize the metallurgical characteristics of Alloy 600. The initial product of this research was a special thermal treatment, performed after final mill anneal to effect intergranular carbide precipitation; this product exhibited enhanced resistance to SCC and was designated thermally treated Alloy 600 (Alloy 600TT). The thermal treatment required that the tubes experience a final mill anneal at a temperature sufficient to dissolve all carbides, followed by a rapid cooldown to room temperature, and subsequent exposure of the alloy in the intergranular precipitation range (approximately 700-725°C) for times sufficient to effect intergranular carbide precipitation and redistribution of the matrix chromium to the regions adjacent to the grain boundaries in order to avoid sensitization. Beginning around 1980, this material dominated steam generator (SG) tubing applications in the U.S., Europe, and Japan for both new and replacement SGs. The performance of these units has been excellent, with an extremely low number of corrosion-related repairs after more than twenty years of service.

The exceptional performance of Alloy 600TT notwithstanding, the nuclear industry continued efforts to optimize SG heat-transfer tubing. This ultimately led, in the late 1980s, to the qualification and selection of thermally treated Alloy 690 (Alloy 690TT). With the exception of German-designed and built PWRs, which use a modified version of Alloy 800 (Alloy 800Mod), all new and replacement SGs placed into service since mid-1989 have been equipped with Alloy 690TT tubes.

The initial choice of Alloy 690TT was the result of a joint effort in the early 1980s between Westinghouse and the French parties Electricité de France, Framatome, and CEA. The corrosion-testing programs that ultimately led to the selection of Alloy 690TT involved long-term exposures at all reasonable and, in some cases, extremely faulted, chemical environments.

These programs evaluated the effects of carbon concentration, final mill annealing and thermal treatment temperatures, and other metallurgical parameters on the corrosion resistance. The results of this research were used to develop procurement specifications for commercial quantities of Alloy 690TT.

2.3 Incoloy 800

Ontario Hydro originally elected to use Alloy 600 at Bruce A and B, based on early PWR experience at the time design decisions were made and because of concerns with early experiments with Alloy 800 which showed that the material was susceptible to cracking in concentrated hydroxide solutions, especially if not made with carefully controlled Ti/C ratio (nuclear grade or "modified" Alloy 800) to prevent sensitization. These early decisions were based on the assumption that SG crevices could become highly alkaline under certain chemistry upset conditions. For CANDU-6 SGs, AECL, after careful review of early Alloy 600 laboratory data showing the susceptibility to PWSCC, and in consultation with developments elsewhere that led to the modified Alloy 800 tubing specification, specified Alloy 800M with a Ti/C ratio >12. This ratio has changed slightly since the late 1970's, but Alloy 800M is used in current CANDU 6 SGs, as well as at Darlington. Current CANDU 6 and Darlington reactors each have four SGs with stainless steel supports and Alloy 800 tubing, with relatively little history of corrosion-related degradation. At Point Lepreau, which has Alloy 800 tubes and uses phosphate water chemistry, pits (including some throughwall pits) have been observed on the hot leg side. The pitting has been attributed to acidic oxidizing conditions.

Although the performance of Alloy 800 tubes in German PWRs has been without incident for over 30 years, recently axial cracking within the tubesheet region of the tube in Biblis has been reported. Also, circumferential cracklike indications attributed to ODSCC have been detected recently in the transition zone at the top of the tubesheet of 29 tubes in the cold leg of Almaraz Unit II in Spain. This is a replacement SG, which has been in operation since 1997. The tubes are made of Alloy 800 with hydraulic expansion.

2.4 Discussion and Conclusions

Although a significant number of SGs in the US have their original mill-annealed Alloy 600 tubes, they are gradually being replaced by either Alloy 600TT or Alloy 690TT. Alloy 800M has been used successfully in Europe and Canada, but not in the US. Both alloys appear to have experienced little stress corrosion related problems so far.

From a design perspective there are several factors to consider when striving for a ≥40 year steam generator life. Perhaps the most important, after good chemistry control (and specifications and equipment to assure this), is the need for a leak-tight condenser. For seawater-cooled sites a titanium-tubed condenser with leak-tight tube-to-tubesheet joints is recommended to minimize any risk of impurity in-leakage, although few utilities have these. It is often assumed that on fresh water sites the condenser requirements can be relaxed, but experience at CANDUs and PWRs indicates that this assumption is false. Although the risk of chloride ingress from lake water in-leakage may be lower, the concentration over time of chloride in steam generator crevices will eventually reach the same levels as seawater in-leakage. Thus leaktight condensers for fresh water-cooled sites should be as high a priority as at seawater-cooled sites.

3. Helical Coil Steam Generator Thermal Hydraulic Model

The helical coil steam generator (HCSG) model has been developed to calculate the heat transfer and pressure drop on both sides of the steam generator. The model is a one-dimensional multi-node design that takes into account the variation of properties of the two fluids and the thermal conductivity of the tube wall with temperature and, where applicable, pressure. Even though the model can be used in several ways for the steam generator design calculations, for this study the inlet conditions (temperature and pressure) as well as the flow rates are defined for both sides, and the desired outlet temperature is specified for the hot (helium) side. The model then iterates on the water flow rate to match the required helium-outlet conditions. If necessary, some steam generator design parameters (namely, the shell diameter and, therefore, number of tubes) are adjusted to achieve the steam outlet temperature close to the design value. The main outputs from the model include the flow rate and outlet temperature on the water side and the pressure drops for both sides. Also, as a result of the calculations, detailed distributions of pressure, temperature, and other parameters (such as heat transfer coefficients) inside the steam generators are also available.

The HCSG model used for this work is based on the helical coil heat exchanger (HCHX) model developed for the thermal analysis of the NGNP IHX (Majumdar et al 2008). The detailed model description is provided in the NGNP IHX report. Limited verification of the HCHX model was carried out by comparing the model predictions against the helical coil heat exchanger designs developed by NGNP vendors.

For this work, the HCHX model was modified to reflect the specific features of the steam generator. These modifications are listed below.

The model was updated to allow the treatment of the two-phase (boiling) region (NGNP IHX model was strictly single phase). The two-phase treatment in the HCHX model generally follows one developed for the analysis of the STAR-LM steam generator (Sienicki and Petkov 2001). Two sub-regions within the boiling region are distinguished – a saturated liquid-continuous region and saturated-vapor-continuous region. In each sub-region, the heat transfer correlations used for the STAR-LM steam generator analysis (Sienicki and Petkov 2001) are adopted for the HCSG model. In accord with the recommendations of Sienicki and Petkov (2001), a transition from liquid-continuous to vapor-continuous flow is assumed to occur at steam quality of 0.99.

For the pressure-drop calculations in the boiling region, a simple homogeneous treatment is used in the HCSG model. Under this approach, the pressure drop is assumed to be equal to that of a single-phase fluid with the properties calculated as quality-averaged properties of the saturated liquid and saturated vapor. This simple treatment is possible because calculation of the pressure drop is not a primary goal for this application of the HCSG model; the pressure drop is used in the model only to predict the variation in the water/steam properties inside the steam generator due to a pressure reduction. As will be shown below, the pressure drop calculated by this simple homogeneous treatment agrees well with the calculations for the NGNP steam generator design (Caspersson. 2009) and such that no refinement of the pressure drop analysis is needed at this time.

In addition to the two-phase flow treatment adopted from the STAR-LM steam generator analysis, a thermal resistance of crud deposits on the water/steam side of the tubes walls is implemented in the HCHX model in the same manner as it is done for STAR-LM (Sienicki and

Petkov 2001). A thermal conductance of 70.9 kW/m^2-K (Sienicki and Petkov 2001) is added to the water-side heat transfer coefficient. In the HCSG model, this additional resistance is added in the boiling region only.

The HCHX model was also updated in this work to allow for the tube materials change inside the steam generator. In previous version of the model, the tube material was assumed to be the same for the entire length of the tubes. In the NGNP SG design (Caspersson 2009), it is proposed to have different tube material (800H) in the superheater region of the steam generator (compared to T22 for the rest of the tube). According to the NGNP SG specifications, the region with the 800H tubes constitutes ≈11% of the entire tube length (35.88 ft out of 316.58 ft of the entire tube length). Since in the HCSG model the steam generator is divided, for calculations, into several nodes along its height, the regions in the upper 11% of the height is assumed to have 800H tube material while the rest of the regions have T22 as a tube material.

The HCSG model also has capabilities to include the design flow margins and the heat loss into the calculations. However, those capabilities have not been used in the current calculations, since it is not clear whether those parameters have been included into the NGNP SG design.

3.1 Results for Thermal Hydraulic Calculations

Table 3.1 shows a comparison of the model results with the design calculations for the NGNP steam generator. Highlighted in yellow are the calculated results while the input parameters are shown in white. Table 3.1 shows two sets of the calculations with the HCSG model. In first calculations (Original), the steam generator geometry, including tube inner and outer diameters, helix angle, number of coils, tube pitches, and so on, is specified as in the design calculations. It is shown in Table 3.1 that HCSG model overpredicted the steam outlet temperature in this case. When the number of coils was reduced (22 coils), very close agreement with the design calculations has been achieved. The results of the calculations suggest that there might be a design margin incorporated into the original steam generator design (no information on the design margin was available to the authors of this report). Table 3.2 shows the calculated coil dimensions for the 22 coils case.

Figure 3.1 shows the results of the calculations in the form of the temperature profiles along the heat exchanger height. Those profiles, along with some other parameters such as heat transfer areas, were supplied in tabulated form for the stress analysis calculations.

Table 3.1. Comparison of the Model Results with NGNP Design

Item		Unit	NGNP design	Model (original)	Model (22 coils)
Unit design heat duty		MW	350		
Design margin		%	N/A	0	0
Heat loss		%	N/A	0	0
Primary side	Fluid		He	He	He
	Side		Shell	Shell	Shell
	Inlet temperature	°C	686.1	686.1	686.1
	Flow rate	kg/s	168.7	168.7	168.7
	Flow rate with margin	kg/s	-	168.7	168.7
	Outlet temperature	°C	283.9	283.9	283.9
	Pressure drop	kPa	7.701	9.107	16.61
	Heat transfer	MW	352.95	352.35	352.35
Secondary side	Fluid		H_2O	H_2O	H_2O
	Side		Tube	Tube	Tube
	Flow rate	kg/s	137.7	126.9	136.8
	Flow rate with margin	kg/s	-	126.9	136.8
	Inlet temperature	°C	193.3	193.3	193.3
	Outlet temperature	°C	540.6	616.3	541.7
	Inlet pressure	MPa	18.17	18.17	18.17
	Pressure drop	kPa	826	607	997
	Heat Transfer	MW	352.95	352.35	352.35
Tube	Outer diameter	mm	22.22	31.8	31.8
	Thickness	mm	3.3	5.9	5.9
	Tube length	m	96.49	96.50	96.50
	Number of tubes		439	441	318
Helically coiled tube bundle	Angle	deg	3.69	3.69	3.69
	Number of coils		28	28	22
	Inner shroud outside diameter	m	1.68	1.68	1.68
	Vessel inside diameter	mm	3.8	3.8	3.35
	Horizontal pitch	mm	38.1	57.2	57.2
	Vertical pitch	mm	35.3	47.6	47.6
	Effective height	m	6.203	6.203	6.203

Color shading: white – input; yellow – calculations.

Table 3.2. Variation of the Parameters by Coils

Coil number	Coil diameter (m)	Number of tubes
1	1.718	10
2	1.794	10
3	1.871	11
4	1.947	11
5	2.023	12
6	2.099	12
7	2.175	12
8	2.252	13
9	2.328	13
10	2.404	14
11	2.480	14
12	2.556	15
13	2.633	15
14	2.709	16
15	2.785	16
16	2.861	16
17	2.937	17
18	3.014	17
19	3.090	18
20	3.166	18
21	3.242	19
22	3.318	19

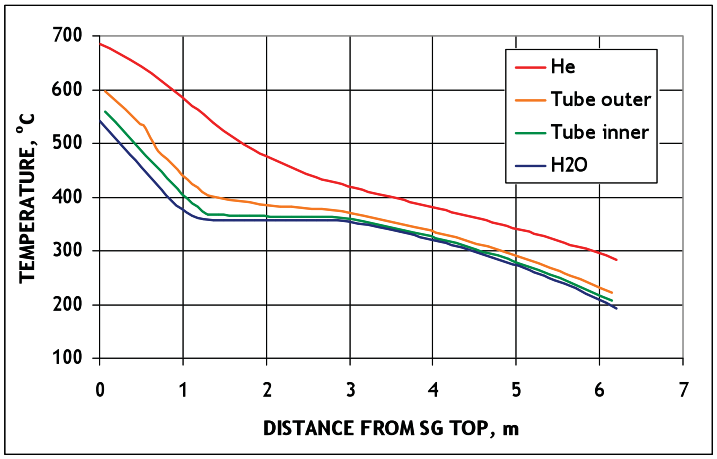

Figure 3.1. Calculated Axial Temperature Profiles for NGNP Steam Generator.

4. Stress Calculations for the Helical Coil Steam Generator

4.1 Introduction

Thermal and stress analyses of a three-dimensional spiral structure like the helical SG are complex. Since its basic component consists of a thin walled tube, the rules of Subsection NH of the ASME Code can be applied. The outer diameter and wall thickness of the tube are 22.2 mm and 3.3 mm, respectively. The average helix, which has a diameter of 2.9 m and is 6.2 m long, consists of approximately ten 360°-turn coils with an axial pitch of 0.65 m. There is a single 360°-turn superheater coil section (Fig. 4.1) integrally attached to the steam generator section. The tube material for the SG is 2-1/4Cr-1Mo and the superheater is made of Alloy 800H. Properties for both materials are provided in Subsection NH of the ASME Code, Section III.

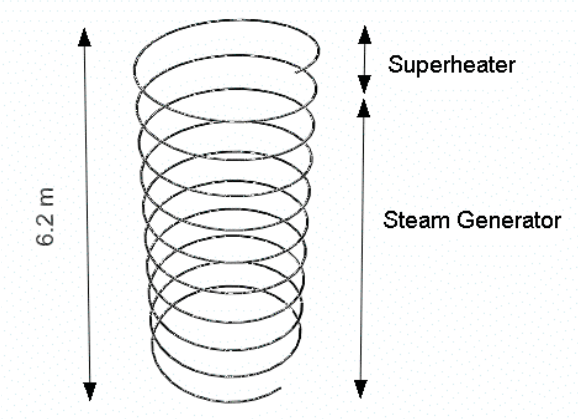

Figure 4.1. Average Helical Coil Steam Generator.

For the purpose of the present report, the superheater (a single 360°-turn coil) and the adjoining single 360°-turn coil of the SG are considered.

4.2 Thermal Conduction Analysis

The heat transfer coefficients (HTCs) and environment temperature data at the inner diameter (ID, water) and the outer diameter (OD, helium) surfaces of the helical SG tube were input in the FEM as functions of vertical (axial) location (Figs. 4.2a-b and 4.3).

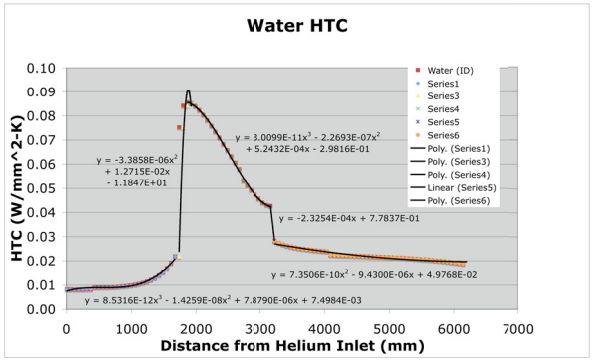

(a)

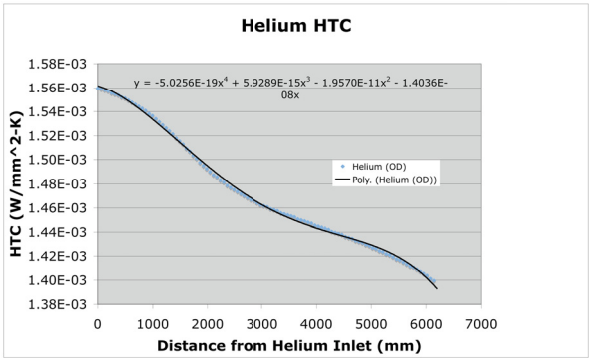

(b)

Figure 4.2. Axial variation of Heat Transfer Coefficients of (a) water and (b) helium

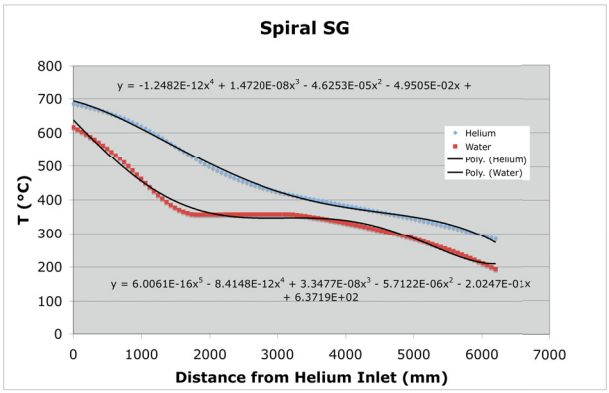

Figure 4.3. Axial variation of water and helium temperatures

The FEA-calculated distribution of temperatures at the hot side (OD surface) of the tube are plotted in Fig. 4.4. The through-thickness temperature variations in the superheater and the SG are plotted in Figs. 4.5a and 4.5b, respectively. The maximum temperatures in the superheater (Alloy 800H) and in the rest of the SG (2-1/4Cr-1Mo) are 659°C and 554°C, respectively.

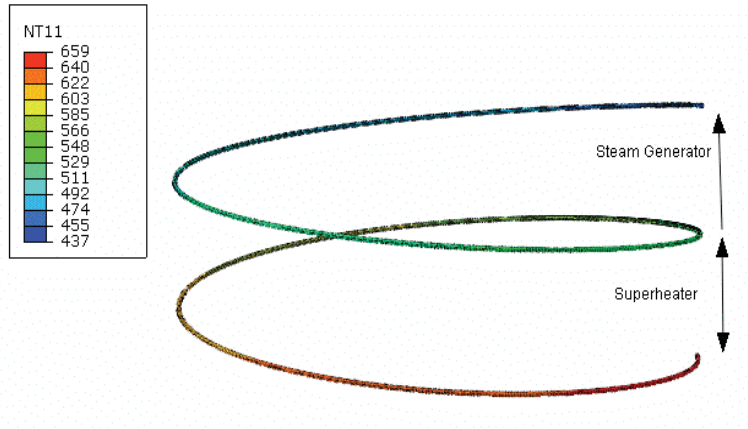

Figure 4.4. Global temperature distribution in the superheater-SG.

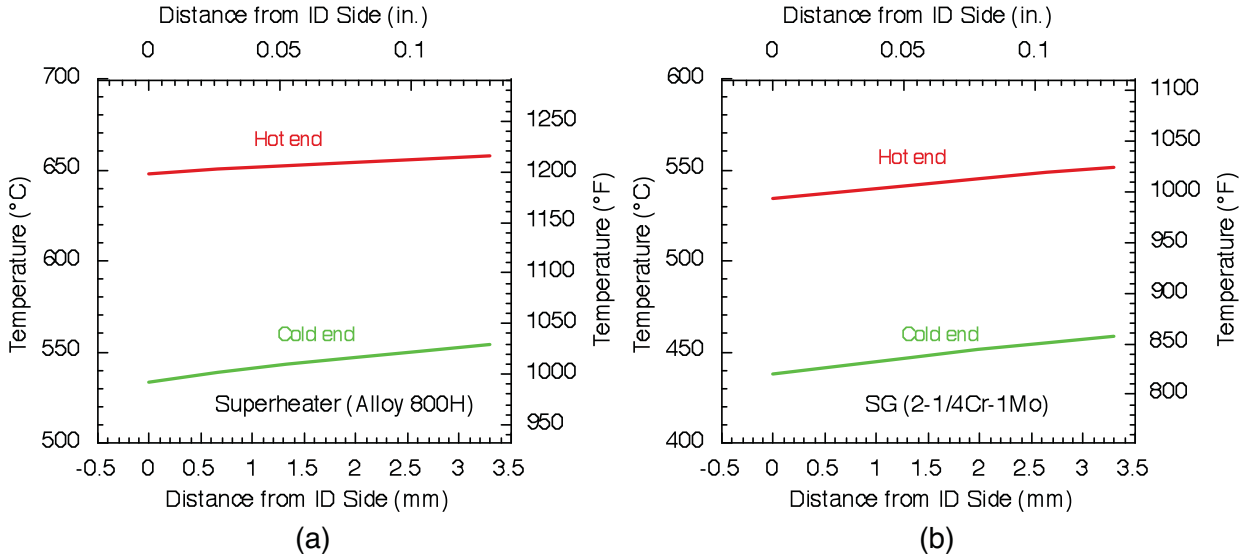

Figure 4.5. Through-thickness temperature distributions in the (a) superheater and (b) SG tubes.

4.3 Stress Analysis

Two stress analyses, both assuming linear elastic behavior, were conducted using the finite element code ABAQUS. First, a primary (pressure) stress analysis was conducted without any contribution from thermal stresses. Second, a secondary (thermal) stress analysis was conducted without the pressure stresses. In the second analysis, the temperature data calculated in the thermal conduction analysis (Section 4.2) were used as input into the ABAQUS code. In all cases, the ends of the helical coil were assumed fixed normal to the coil section and the helix was allowed to deform radially without any constraint. To prevent rigid body translations and rotations of the helix, a sufficient number of transverse degrees of freedom were constrained at the ends so that a uniform temperature rise of the helix could be accommodated without stress.

4.3.1 Primary Stress Analysis

The pressure of the helium on the OD surface was constant at 7 MPa and water pressure on the ID surface was constant at 18 MPa. The stress distribution through the thickness of the tube wall is constant along the axis of the helical SG (Fig. 4.6) as well as in the azimuthal direction of the tube at any axial location of the helix (Fig. 4.7).

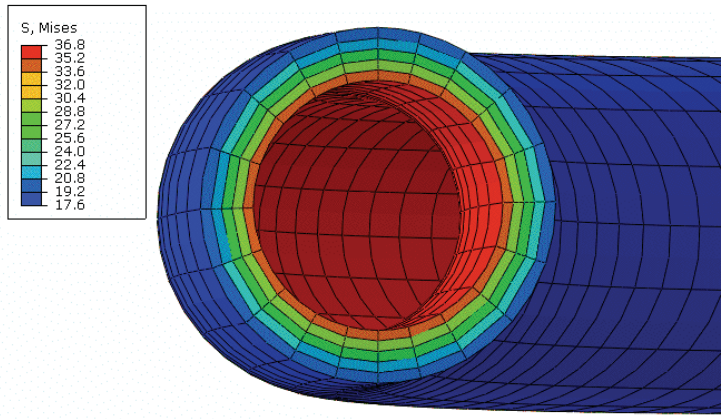

Figure 4.6. Von Mises stress distribution in the helical SG and superheater.

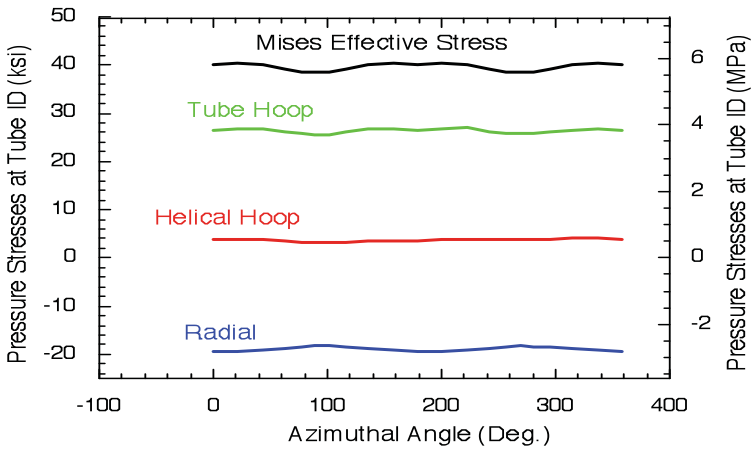

Figure 4.7. Azimuthal (tube hoop) distributions of primary stress components and the Von Mises effective stress at the tube OD surface at any axial location of the helical SG and the superheater.

The distributions of the various stress components through the thickness of the tube wall are shown in Fig. 4.8. The general primary membrane stress intensity P_m is 28 MPa and the local primary membrane plus bending stress intensity P_L+P_b = 40 MPa.

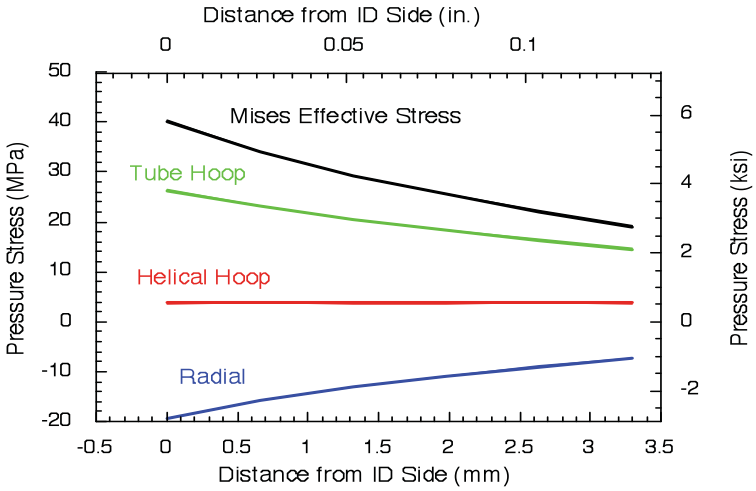

Figure 4.8. Through-thickness distributions of primary stress components and the Von Mises effective stress in the helical SG and the superheater.

4.3.2 Secondary Stress Analysis

The distribution of thermal stress near the hot end of the superheater is plotted in Fig. 4.9. The azimuthal variation of the stress is uniform. However, the stresses vary in the thickness direction of the tube as well as the axial direction of the helix. Through-thickness stress distribution in the superheater at the hot end and near the cold end slightly away from the joint are plotted in Figs. 4.10a and 4.10b, respectively. The stresses at the cold end at the exact location of the Alloy 800H-to-2-1/4Cr-1Mo joint are peaked because of incompatibility of mechanical properties between the two materials. The stress levels at the cold end are higher than those at the hot end because both the Young's modulus and the temperature drop through the wall at the cold end are greater than those at the hot end.

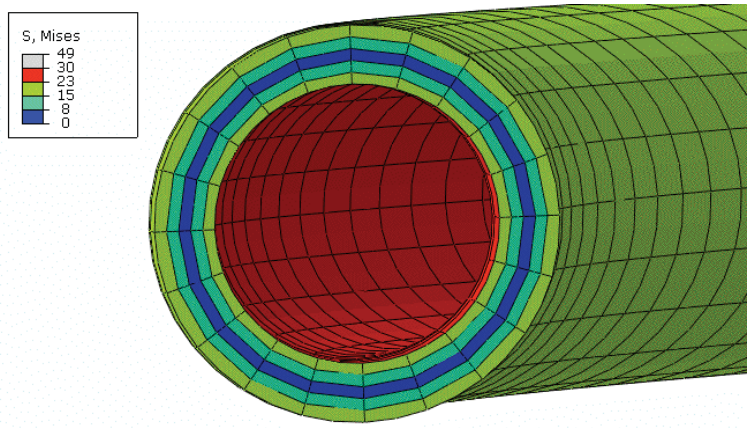

Figure 4.9. Distribution of Von Mises effective thermal stress at the hot end of the superheater.

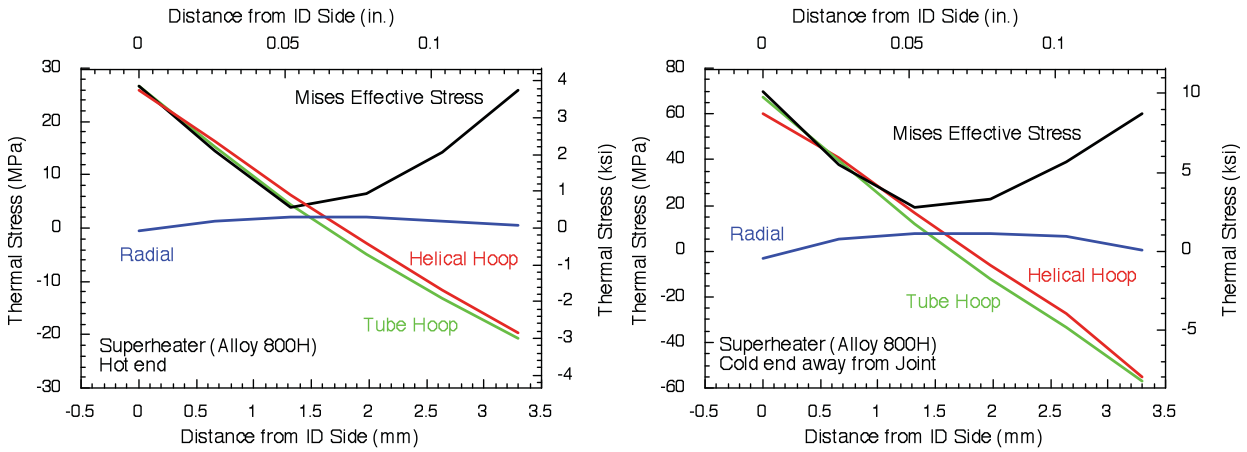

Figure 4.10. Through-thickness thermal stress distribution in the superheater at (a) hot end and (b) cold end.

Through-thickness stress distribution in the SG near the hot end slightly away from the joint and at the cooler end are plotted in Figs. 4.11a and 4.11b, respectively. Note that the stresses at the two ends are similar because the temperature drops through the thickness are simlar. The maximum Von Mises effective thermal stress is 50 MPa.

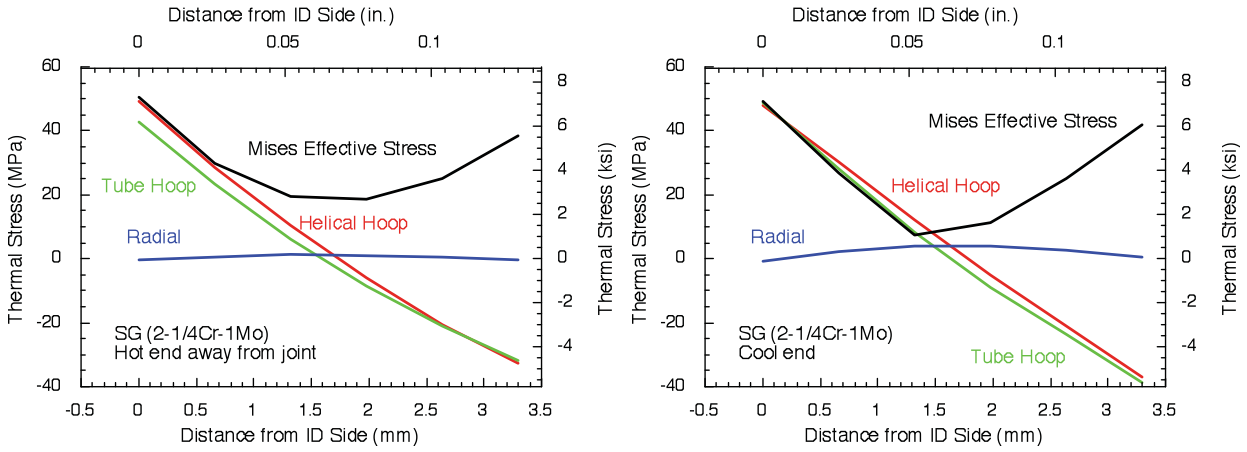

Figure 4.11. Through-thickness thermal stress distribution in the SG at (a) hot end and (b) cool end.

As mentioned earlier, the mismatch in mechanical properties of Alloy 800H and 2-1/4Cr-1Mo creates a peaking of the stress at the junction. A peak stress of 120 MPa is created at the junction, as shown in Fig. 4.12.

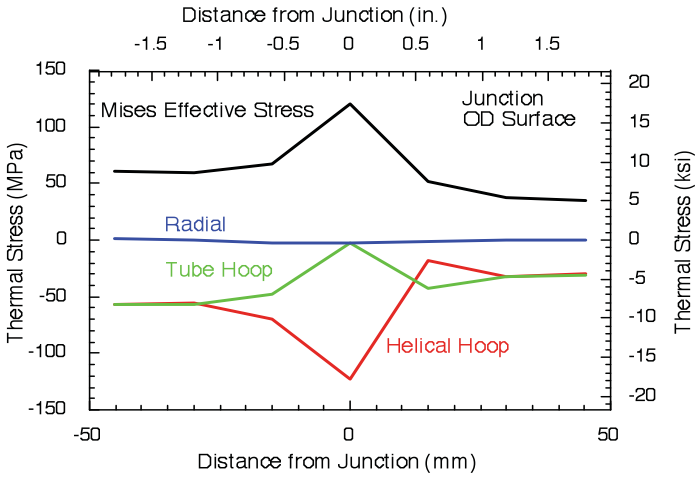

Figure 4.12. Variation of the thermal stress components at the tube OD surface near the dissimilar material joint.

4.3.3 ASME Code Compliance Calculations

Both Alloy 800H and 2-1/4Cr-1Mo steel are approved for high temperature use as per Subsection NH of the ASME Code, Section III.

Primary Stress Limits

A basic high temperature primary stress limit is S_{mt}, which is the lesser of S_m and S_t, and is a function of both time and temperature. For nickel-based alloys, S_m is defined basically as follows:

$$S_m = \min \begin{cases} \frac{1}{3} S_u \\ \frac{2}{3} S_y \end{cases} \qquad (4.1)$$

where S_u is the lesser of ultimate tensile strength at temperature and the minimum ultimate tensile strength at room temperature, S_y is the lesser of yield strength at temperature and the minimum yield strength at room temperature. For each specific time t and temperature T, S_t is defined as the least of the following three stresses:

(1) 100% of average stress required to obtain a total (elastic, plastic, and creep) strain of 1%,
(2) 80% of the minimum stress to cause initiation of tertiary creep, and (4.2)
(3) 67% of the minimum stress to cause rupture.

The variations of S_{mt} with time and temperature for Alloy 800H and 2-1/4Cr-1Mo are plotted in Figs. 4.13a and 4.13b, respectively. The symbols in these figures represent the general primary membrane stress intensities (P_m), primary membrane plus bending stress intensities (P_L+P_b) and average temperatures of the wall of the superheater and the SG. Figure 4.13a shows that the allowable design life (creep rupture) for the superheater (Alloy 800H) is ≈3 X 10^5 h. However, the allowable design life (creep rupture) for the SG is ≈10^5 h (Fig. 4. 13b).

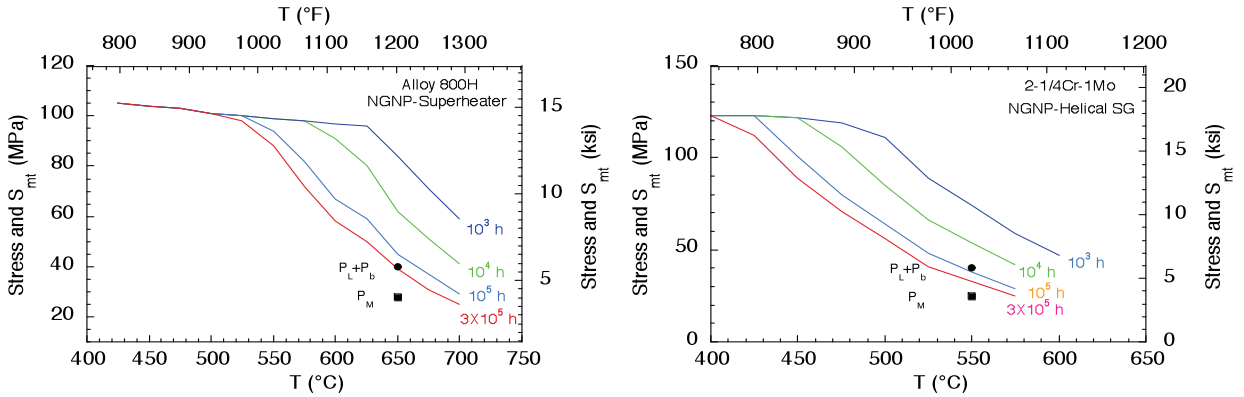

Figure 4.13. Variation of S_{mt} with time and temperature for (a) Alloy 800H and (b) 2-1/4Cr-1Mo. Also shown by symbols are the points representing the average primary membrane stress intensities (P_m), primary membrane plus bending stress intensities (P_L+P_b) and average wall temperatures for the superheater and the SG.

Primary Plus Secondary Stress Limit

Ratcheting Limit

One of the available tests in Subsection NH for satisfying the ratcheting strain limit is Test no A2 for those cycles during which the average wall temperature at one of the stress extremes defining the maximum cyclic primary plus secondary stress range is below the temperature where creep is negligible.

Test No. A2

$$X + Y \leq 1 \qquad (4.3)$$

In Eq.(4.3), $X=(P_L + P_b)/S_y$ or P_m/S_y and $Y=Q/S_y$ where Q=secondary stress intensity range, and S_y is the average of the yield strengths at the maximum and minimum wall-averaged temperatures during the cycle. The relevant quantities are given in Tables 4.1 and 4.2, needed for ratcheting analyses of the superheater and the SG, respectively.

Assuming that the low temperature end of the temperature cycle is below the creep range, it can be verified that Test No. A2 (Eq. 4.3) is satisfied for both locations considered in Tables 4.1 and 4.2.

Table 4.1. Summary of primary and secondary stresses in helical SG superheater (Alloy 800H) at the cold and hot ends.

Location	$P_L + P_b$ (MPa)	Q (MPa)	T (°C) Max	T (°C) Min	S_y (MPa)	X	Y
Cold end	40	70	550	300	160	0.25	0.44
Hot end	40	27	660	300	155	0.26	0.17

Table 4.2. Summary of primary and secondary stresses in the helical SG (2-1/4Cr-1Mo) at the cold and hot ends of the hottest 360°-turn coil.

Location	$P_L + P_b$ (MPa)	Q (MPa)	T (°C) Max	T (°C) Min	S_y (MPa)	X	Y
Cold end	40	50	450	300	185	0.22	0.27
Hot end	40	50	550	300	184	0.22	0.27

Creep-Fatigue Limit

Creep-fatigue was not considered in this report. However, the peak stress (Fig. 4.12) created at the junction between the Alloy 800H and 2-1/4Cr-1Mo is a potential source for creep-fatigue damage and needs a detailed analysis.

5. Summary

Thermal conduction and basic pressure and thermal stress analyses of two of the hottest 360°-turn coils of the SG/superheater have been conducted. The stresses have been compared to the allowables of Subsection NH of the ASME Code. The primary stresses in the Alloy 800H superheater limit its creep rupture design life to 3×10^5 h. The primary stresses in the 2-1/4Cr-1Mo SG limit its creep rupture design life to 10^5 h. Both the SG and the superheater satisfy the ratcheting strain limit of Subsection NH.

There is significant peaking of the stresses at the joint between the 2-1/4Cr-1Mo and Alloy 800H tubes. These stresses have to be investigated in detail for possible creep-fatigue damage.

In future, all the coils of the SG need to be included in the FEM. Their inclusion would lower the highest temperatures calculated for the coils in the present report since it would allow heat conduction to occur in the axial direction of the helix. However, the effect should be small because convective heat transfer through the coolant dominates the conductive heat transfer through the tube wall.

6. References

Berry, W. E., O. M. Stewart, and F. W. Fink, 1960, Examination of a Nonregenerative Heat Exchanger from the USS Nautilus (SNN–571), BMI–1416, Battelle Memorial Institute.

Bush, S. H., and R. L. Dillon, 1973, Stress Corrosion in Nuclear Systems, CONF–730605–2, Battelle Northwest Laboratory.

Caspersson, S., 2009, Helium Steam Generator Development Status Summary, Westinghouse Electric Company.

Cheng, C. F., 1975, Intergranular Stress–Assisted Corrosion Cracking of Austenitic Alloys in Water–Cooled Nuclear Reactors, J. Nucl. Mater., Vol. 56, pp. 11–33.

Copson, H. R., and W. E. Berry, 1962, Corrosion of Inconel Nickel-Chromium Alloy in Primary Coolants of Pressurized Water Reactors, Corrosion, Vol. 18, pp. 21t-26t.

Coriou, H., L. Grall, C. Mahieu, and M. Pelas, 1959, Sensitivity to Stress Corrosion and Intergranular Attack of High-Nickel Austenitic Alloys, Corrosion, Vol. 22 (1966), pp. 280-290. Coriou's first paper (in French) Corrosion Fissurante Sous Contrainte De L'Inconel Dans L'Eau a Haute Temperature, appeared in 3rd Colloque de Metallurgie - Corrosion, Centre D'Etudes Nuclearies de Saclay.

Gras, J. M., 1992, Stress Corrosion Cracking of Steam Generator Tubing Materials, in Proc. Parkins Symp. on Fundamental Aspects of Stress Corrosion Cracking, S. M. Bruemmer et al., eds., The Minerals, Metals, & Materials Society, Warrendale, PA, pp. 411–432.

Green, S. J. and J. P. N. Paine, 1981, Materials Performance in Nuclear Pressurized Water Reactor Steam Generators, Nucl. Technol., Vol. 55, pp. 10-29.

Harrod, D. L., R.E. Gold, and R.J. Jacko, 2001, Alloy Optimization for PWR Steam Generator Heat-Transfer Tubing, J. of Materials, Light Water Reactors Overview.

Karwoski, K. J., G. L. Makar and M. G. Yoder, 2007, U.S. Operating Experience with Thermally Treated Alloy 690 Steam Generator Tubes, NUREG-1841.

Kratzer, W. K., 1971, 304 Stainless Steel Steam Generator Tube Experience at N–Reactor, DUN–SA–178, DuPont Co., Wilmington, DE.

LaQue, F. L., 1957, Personal communication, as reported by W. L. Williams and J. F. Eckel in, Corrosion and Wear Handbook for Water Cooled Reactors, Chapter 10, D. J. Paul, ed., USAEC TID 7006, pp. 117,165.

Majumdar, S., A. Moisseytsev, and K. Natesan, 2008, Assessment of the Next Generation Nuclear Plant Intermediate Heat Exchanger Design, ANL/EXT-08-32, Argonne National Laboratory.

Majumdar, S., 1999, Assessment of Current Understanding of Mechanisms of Initiation, Arrest, and Reinitiation of Stress Corrosion Cracks in PWR Steam Generator Tubing, NUREG/CR-5752 ANL-99/4, Argonne National Laboratory, IL.

McKane, R. H., H. C. Minton, and J. W. Wade, 1960, Stainless Steel Failure in Savannah River Plant Reactor Areas, DP–539, DuPont Co., Wilmington, DE.

Paine, J. P. N., R. S. Pathania, and C. E. Shoemaker, 1988, Effect of Caustic Environment on Intergranular Attack and Stress Corrosion Cracking of Alloy 600, Proc. 3rd Int. Symp. on Environmental Degradation of Materials in Nuclear Power Systems—Water Reactors, Traverse City, MI, The Metallurgical Society/AIME, Warrendale, PA, pp. 501-509.

PWR primary water chemistry guidelines: Revision 2, 1990, EPRI NP-7077, Final report, Electric Power Research Institute, Palo Alto, CA.

PWR secondary water chemistry guidelines - Revision 3, 1993, prepared by Secondary Water Chemistry Guidelines Revision Committee, EPRI-TR-102134, Electric Power Research Institute, Palo Alto, CA.

Sienicki, J. J. and P. V. Petkov, “Operational and Passive Safety Aspects of the STAR-LM Natural Convection HLMC Reactor – Study on Operational Aspects of a Natural Convection HLMS Reactor (II),” Argonne National Laboratory, September 2001.

Singley, W. J., I. H. Welinsky. S. F. Whirl, and H. A. Klein, Stress Corrosion of Stainless Steel and Boiler Water Treatment at Shippingport Atomic Power Station, pp. 748–768 in Proc. Amer. Power Conf., Vol. XXI (1959).

Steam Generator Owners Group, Steam Generator Reference Book, Electric Power Research Institute, Palo Alto, CA (1985).

Steam Generator Progress Report; EPRI report TR-106365-R15 (2000).

Steam Generator Reference Book, EPRI TR-103824 (Dec. 1994).

Tapping, R., "Steam Generator Aging in CANDUS: 30 Years of Operation and R&D," Presented at the 5th CNS International Steam Generator Conference, Toronto, Ontario, Canada November 26 - 29, 2006.

Wagner, H. A., Light Water Reactor Experience in the United States of America, pp. 503–520 in Performance of Nuclear Power Reactor Components, CONF–691115, International Atomic Energy Agency, Vienna (1970).

Welinsky, I. H., W. F. Brindley, W. E. Berry, and S. F. Whirl, Final Evaluation of Shippingport Power Station’s Stainless Steel Generator after Five Years, pp. 1–13 in Proc. Symp. on High Purity Water Corrosion of Metals, 23rd NACE Conf., National Association of Corrosion Engineers, Houston, TX (1968).

Welty, C. S. Jr. and J. C. Blomgren, Steam Generator Issues, Proc. of the Fourth Int. Symp. on Environmental Degradation of Matls. in Nuclear Power Systems - Water Reactors, Ed. D. Cubicciotti, ed., NACE, Houston, TX (1990), pp. 1-27,1-36.